

Article

Antitumor Activities against Breast Cancers by an Afucosylated Anti-HER2 Monoclonal Antibody H₂Mab-77-mG_{2a}-f

Tomohiro Tanaka ¹, Hiroyuki Suzuki ^{1,2,*}, Tomokazu Ohishi ^{3,4}, Mika K. Kaneko ^{1,2}, Yukinari Kato ^{1,2,*}

¹ Department of Molecular Pharmacology, Tohoku University Graduate School of Medicine, 2-1 Seiryomachi, Aoba-ku, Sendai 980-8575, Miyagi, Japan; tomohiro.tanaka.b5@tohoku.ac.jp (T.T.); k.mika@med.tohoku.ac.jp (M.K.K.)

² Department of Antibody Drug Development, Tohoku University Graduate School of Medicine, 2-1 Seiryomachi, Aoba-ku, Sendai 980-8575, Miyagi, Japan

³ Institute of Microbial Chemistry (BIKAKEN), Numazu, Microbial Chemistry Research Foundation, 18-24 Miyamoto, Numazu-shi 410-0301, Japan; ohishit@bikaken.or.jp (T.O.)

⁴ Institute of Microbial Chemistry (BIKAKEN), Laboratory of Oncology, Microbial Chemistry Research Foundation, 3-14-23 Kamiosaki, Shinagawa-ku 141-0021, Tokyo, Japan

* Correspondence: hiroyuki.suzuki.b4@tohoku.ac.jp (H. S.); yukinari.kato.e6@tohoku.ac.jp (Y.K.); Tel.: +81-22-717-8207 (H.S., Y.K.)

Abstract: Breast cancer patients with high levels of HER2 (human epidermal growth factor receptor 2) expression had worse clinical outcomes. Anti-HER2 monoclonal antibody (mAb) is the most important therapeutic modality for HER2-positive breast cancer. We previously immunized mice with the ectodomain of HER2 to create the anti-HER2 mAb, H₂Mab-77 (mouse IgG₁, kappa). This was then altered to produce H₂Mab-77-mG_{2a}-f, an afucosylated mouse IgG_{2a}. In the present work, we examined the reactivity of H₂Mab-77-mG_{2a}-f and antitumor effects against breast cancers *in vitro* and *in vivo*. BT-474, an endogenously HER2-expressed breast cancer cell line, was identified by H₂Mab-77-mG_{2a}-f with a strong binding affinity [a dissociation constant (K_D): 5.0×10^{-9} M]. H₂Mab-77-mG_{2a}-f could stain HER2 of breast cancer tissues in immunohistochemistry and detect HER2 protein in western blot analysis. Furthermore, H₂Mab-77-mG_{2a}-f demonstrated strong antibody-dependent cellular cytotoxicity (ADCC) and complement-dependent cytotoxicity (CDC) for BT-474 cells. MDA-MB-468, a HER2-negative breast cancer cell line, was unaffected by H₂Mab-77-mG_{2a}-f. Additionally, in the BT-474-bearing tumor xenograft model, H₂Mab-77-mG_{2a}-f substantially suppressed tumor development when compared to the control mouse IgG_{2a} mAb. In contrast, the HER2-negative MDA-MB-468-bearing tumor xenograft model showed no response to H₂Mab-77-mG_{2a}-f. These findings point to the possibility of H₂Mab-77-mG_{2a}-f as a treatment regimen by showing that it has antitumor effects on HER2-positive breast tumors.

Keywords: HER2; monoclonal antibody; ADCC; CDC; antitumor activity

1. Introduction

The receptor tyrosine kinase human epidermal growth factor receptor 2 (HER2, also known as ERBB2) is a type I transmembrane glycoprotein that controls cell development and survival. HER2 can form homodimer and heterodimers with related family members including EGFR, HER3, and HER4. The complexes initiate intracellular signaling pathways like mitogen-activated protein kinase and phosphoinositide 3-kinase/Akt (PI3K/Akt). The extracellular domain of HER2 is composed of four regions, domain I to IV. Unlike other family receptors, HER2 extracellular domain basically has an active structure, dimer formation with other molecules is possible even without a ligand [1,2]. This structural characteristic is assumed to be the root of HER2's lack of ligand basis [3]. It should be

mentioned that HER2 and HER3 interactions create extremely potent mitogenic signals and have been implicated in cancer progression [4–6].

The most frequent kind of cancer among women is breast cancer [7]. 43,170 American women will pass away from breast cancer in 2023, according to 297,790 new cases [7]. 20% of breast cancer patients have an overexpression of HER2, which is linked to a poor prognosis [8–11]. Carcinogenic HER2 activation is caused by a change in the HER2 receptor gene, more HER2 overexpression and amplification, and less phosphatase activity [12]. Breast tumor incidence and development are correlated with HER2 gene amplification and protein overexpression; this was discovered in 1987 [13]. Angiogenesis, cell cycle progression, survival, angiogenesis, migration, invasion, and tumorigenesis are all accelerated by aberrant activation of HER2 [14–17]. Breast cancer brain metastases are among the cancer subtypes with an elevated risk of HER2-amplified tumors [18,19]. In order to forecast the effectiveness of anti-HER2 therapy, immunohistochemistry and/or in situ hybridization are often used to evaluate the HER2 status of breast cancer [20]. The development of HER2-targeted medicines has advanced significantly, and HER2 has grown in popularity as a cancer therapeutic target [21].

Trastuzumab emtansine (T-DM1) and trastuzumab deruxtecan (T-DXd) are antibody-drug conjugates (ADCs) in which the payload is attached to trastuzumab, a humanized anti-HER2 monoclonal antibody (mAb) [22–24]. Trastuzumab has been used to treat HER2-positive metastatic breast cancer. T-DM1 was authorized for HER2-positive advanced breast cancer by the US Food and Drug Administration (FDA) and the European Medicines Agency in 2013, while T-DXd was approved in the US in 2019 for HER2-positive metastatic or unresectable breast cancer [25–27]. Trastuzumab binds to HER2 domain IV, causing antibody-dependent cellular cytotoxicity (ADCC), antibody-dependent cell phagocytosis (ADCP), HER2 internalization-mediated destruction, and dimerization inhibition [28–30]. The extracellular domain of HER2 has been seen in breast cancer patients' serum, but trastuzumab binding prevents this HER2 cleavage [31,32]. After connecting to the receptors, the ADCs are internalized by endocytosis, where they eventually release their payloads and cause cell damage. As a result, trastuzumab-based ADCs are potent weapons that combine the dual antitumor action of trastuzumab with a cytotoxic payload. T-DM1 has been shown to preserve trastuzumab effects such as blocking HER2 ectodomain cleavage, inhibiting PI3K/Akt signaling, and engaging immune cells through Fc-gamma (Fc γ) receptors, resulting in ADCC [33]. T-DXd is an ADC of the future that combines deruxtecan and trastuzumab. Due to the bystander impact of its potent payload on surrounding cells, T-DXd has been found to be effective not only on HER2-high tumor cells but also on HER2-low tumor cells [26,34]. T-DXd is being tested in clinical studies to see whether it can be used to treat HER2-positive gastric and non-small-cell lung cancer [35,36].

Targeting different HER2 epitopes may make it easier to stop HER2-dependent cell growth, which would stop the growth of tumors [37]. Pertuzumab, a therapeutic antibody authorized in 2012 for HER2-positive breast cancer, binds to the domain II of HER2, preventing receptor dimerization with partner receptors and related signal transduction [38–40]. Pertuzumab, although having ADCC efficacy equal to trastuzumab, does not decrease HER2 shedding [31,40,41]. A potential mechanism for resistance to anti-HER2 therapy includes alteration of the HER2 ectodomain, which results in a reduction of anti-HER2 antibody binding affinity [42]. Anti-HER2 treatments using distinct anti-HER2 mAb variants, such as binding epitopes, or in conjunction with chemotherapy might pave the way for the continued development of HER2-targeted cancer therapies.

We previously created an anti-HER2 mAb (clone H₂Mab-77; mouse IgG₁, kappa) by immunizing mice with the ectodomain of HER2 or with LN229 glioblastoma cells that overexpress HER2 [43]. Flow cytometry, western blotting, and immunohistochemical tests may all be performed with H₂Mab-77. To test its ADCC, complement-dependent cytotoxicity (CDC), and antitumor efficacy in xenograft models, we also altered H₂Mab-77 into a core-fucose-deleted and subclass-converted anti-HER2 mAb (H₂Mab-77-mG_{2a}-f). The activation of natural killer cells (NK cells), which is enhanced by the antibody's Fc region binding to Fc γ RIIIa on NK cells, results in the destruction of target cells, including tumor cells, and facilitates ADCC [44]. A core-fucose deletion in the Fc N-glycan has been shown to improve the binding of Fc to Fc γ RIIIa on effector NK cells [45,46]. In this work, we assessed

the antitumor efficacy of H₂Mab-77-mG_{2a}-f against breast cancer using *in vitro* and *in vivo* models, as well as its reactivities in flow cytometry, western blotting, and immunohistochemical investigations.

2. Results

2.1. Development of a Core-Fucose-Deficient Anti-HER2 mAb, H₂Mab-77-mG_{2a}-f

We previously created an anti-HER2 mAb, H₂Mab-77 (mouse IgG₁, kappa), by immunizing mice with either the HER2 ectodomain or LN229 glioblastoma cells overexpressing HER2. Flow cytometry, western blotting, and immunohistochemical tests revealed that H₂Mab-77 has a high binding affinity.

In this study, we changed the antibody to improve its antitumor efficacy. We altered the subclass of H₂Mab-77 from mouse IgG₁ to mouse IgG_{2a} by joining the V_H and V_L chains of H₂Mab-77 with the C_H and C_L chains of mouse IgG_{2a}, respectively, since mouse IgG₁ has no ADCC and CDC activity. In addition, utilizing BINDS-09 cells (ExpiCHO-S cells lacking FUT8 fucosyltransferase), an afucosylated mouse IgG_{2a} form of H₂Mab-77 (H₂Mab-77-mG_{2a}-f) was generated (Figure 1).

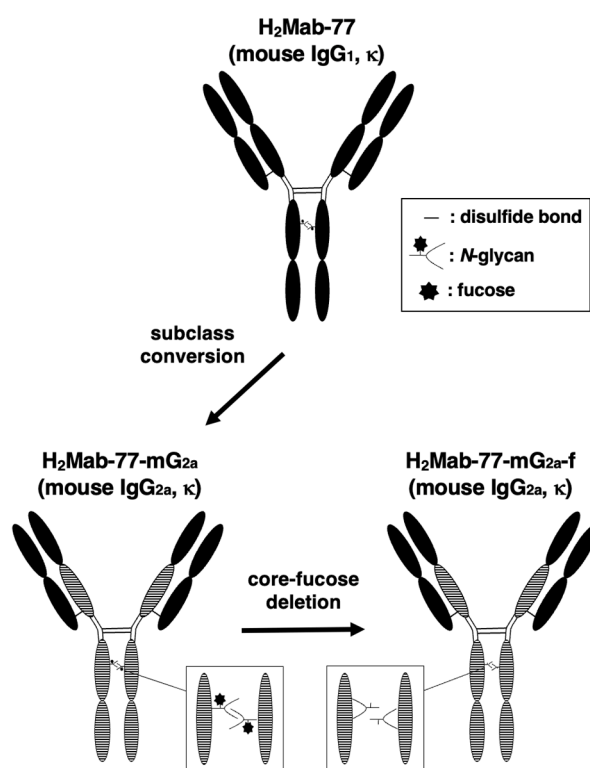


Figure 1. Generation of H₂Mab-77-mG_{2a}-f (mouse IgG_{2a}) and H₂Mab-77-mG_{2a}-f (core-fucose-deleted mouse IgG_{2a}) from the original anti-HER2 mAb, H₂Mab-77 (mouse IgG₁).

2.2. Analysis of H₂Mab-77-mG_{2a}-f Reactivity against Breast Adenocarcinoma Cells by Flow Cytometry

In a previous study, the original H₂Mab-77 (mouse IgG₁, kappa) was found to be suitable for flow cytometry, western blotting, and immunohistochemistry [43]. In this study, an afucosylated form of the anti-HER2 mAb, H₂Mab-77-mG_{2a}-f, was generated. Similar to the original H₂Mab-77, H₂Mab-77-mG_{2a}-f successfully detected exogenously overexpressed HER2 in LN229 (LN229/HER2 cells) at 1 or 10 µg/mL (Figure 2A,B).

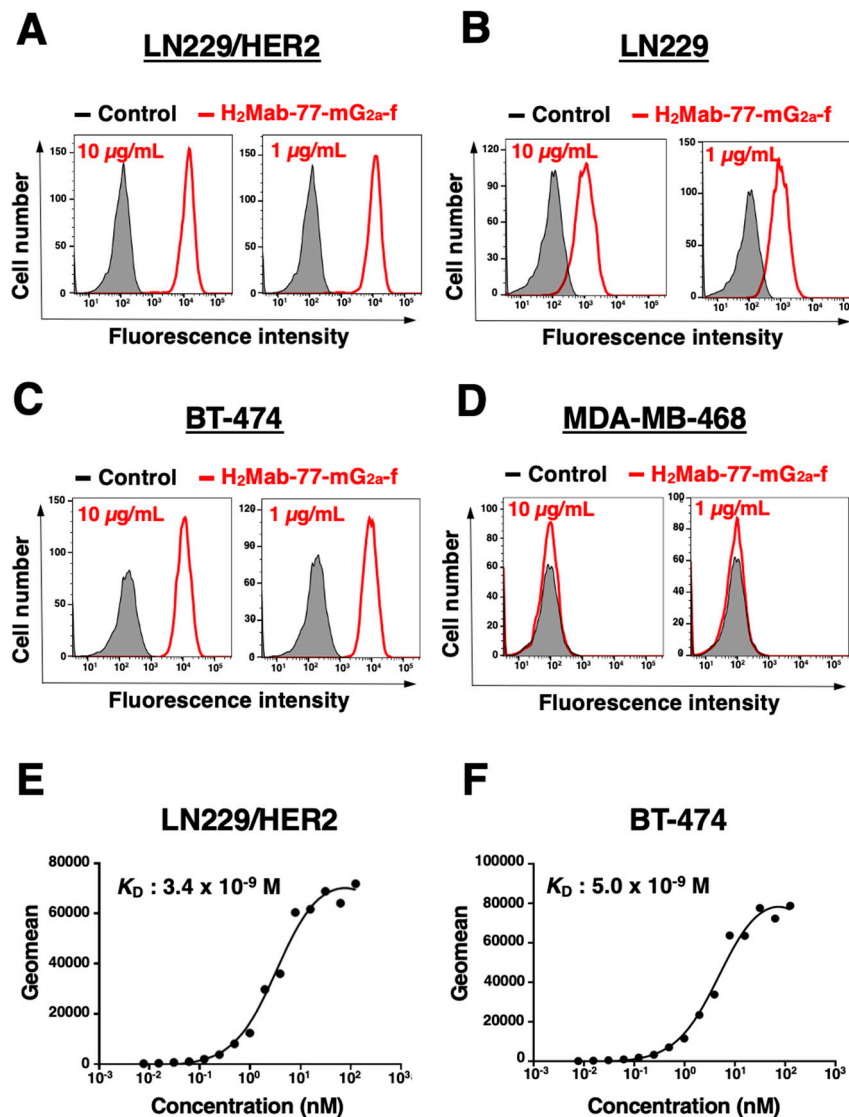


Figure 2. Flow cytometric analysis using H₂Mab-77-mG_{2a-f}. (A) LN229/HER2, (B) LN229, (C) BT-474, and (D) MDA-MB-468 cells were treated with H₂Mab-77-mG_{2a-f} (red) or buffer control (black), followed by Alexa Fluor 488-conjugated anti-mouse IgG. Fluorescence data were analyzed using the SA3800 Cell Analyzer. The binding affinity of H₂Mab-77-mG_{2a-f} was determined by flow cytometry in (E) LN229/HER2 and (F) BT-474 cells. Serially diluted H₂Mab-77-mG_{2a-f} was added to the cells, followed by Alexa Fluor 488-conjugated anti-mouse IgG. Fluorescence data were collected using the SA3800 Cell Analyzer, and the dissociation constant (K_D) was calculated using GraphPad PRISM 6.

Next, we conducted flow cytometric analysis using H₂Mab-77-mG_{2a-f} on two breast cancer cell lines, BT-474 and MDA-MB-468. BT-474 represents the luminal B type of breast cancer with positive expression of progesterone receptor (PR⁺), estrogen receptor (ER⁺), and HER2. In contrast, MDA-MB-468 is a triple-negative breast cancer lacking expression of PR, ER, and HER2 [47]. H₂Mab-77-mG_{2a-f} demonstrated recognition of endogenously expressed HER2 in BT-474 at 1 or 10 µg/mL, while it showed no response to MDA-MB-468 at either concentration (Figure 2C,D).

Subsequently, we evaluated the binding affinity of H₂Mab-77-mG_{2a-f} to LN229/HER2 cells and BT-474 cells using flow cytometry. The apparent dissociation constants (K_D) of H₂Mab-77-mG_{2a-f} to LN229/HER2 and BT-474 cells were determined to be 3.4×10^{-9} M and 5.0×10^{-9} M, respectively (Figure 2E,F). These findings indicate that H₂Mab-77-mG_{2a-f} can effectively recognize HER2 in both cell types with a high binding affinity.

2.3. Western Blotting Using H₂Mab-77-mG_{2a-f}

Similar to the original H₂Mab-77, H₂Mab-77-mG_{2a-f} detected the HER2 band with an estimated 180-kDa band in lysates generated from LN229, LN229/HER2, and BT-474 cells; no band was seen in MDA-MB-468 cells, which are HER2-negative (Figure 3A). For the internal control, an anti-IDH1 mAb (clone RcMab-1) was employed (Figure 3B). These findings revealed that H₂Mab-77-mG_{2a-f} may be employed in western blotting to assess HER2 expression in cultured cells, including breast cancer cells.

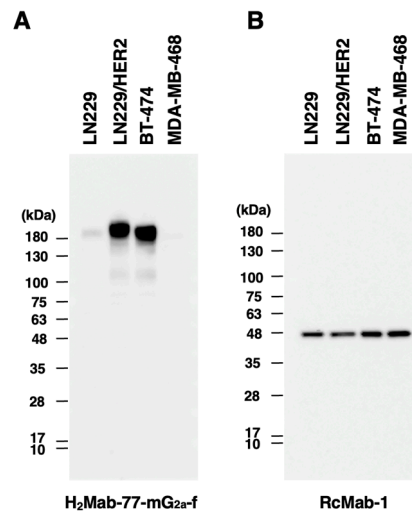


Figure 3. Detection of HER2 by western blotting using H₂Mab-77-mG_{2a-f}. Cell lysates were electrophoresed and transferred onto PVDF membranes. After blocking, the PVDF membranes were incubated with H₂Mab-77-mG_{2a-f} (1 μ g/mL) (A) or an anti-IDH1 monoclonal antibody (clone RcMab-1, 1 μ g/mL) (B), followed by incubation with peroxidase-conjugated anti-mouse immunoglobulins or peroxidase-conjugated anti-rat immunoglobulins. Blots were developed using ImmunoStar LD or ECL Plus Western Blotting Substrate and imaged with a Sayaca-Imager.

2.4. Immunohistochemical Analyses Using H₂Mab-77-mG_{2a-f} against Breast Cancer Tissue

The H₂Mab-77-mG_{2a-f} antibody was then utilized to target clinical specimens of human breast cancer tissue array via immunohistochemistry analysis. Similar to the original H₂Mab-77, H₂Mab-77-mG_{2a-f} identified HER2 on the plasma membrane of breast cancer tissue (Figure 4). Table 1 summarizes the immunohistochemical study of breast cancer. H₂Mab-77-mG_{2a-f} effectively stained HER2 in 14 of 63 cases (22%) of breast cancer, showing its use in the immunohistochemical investigation of formalin-fixed paraffin-embedded tumor sections for identifying HER2.

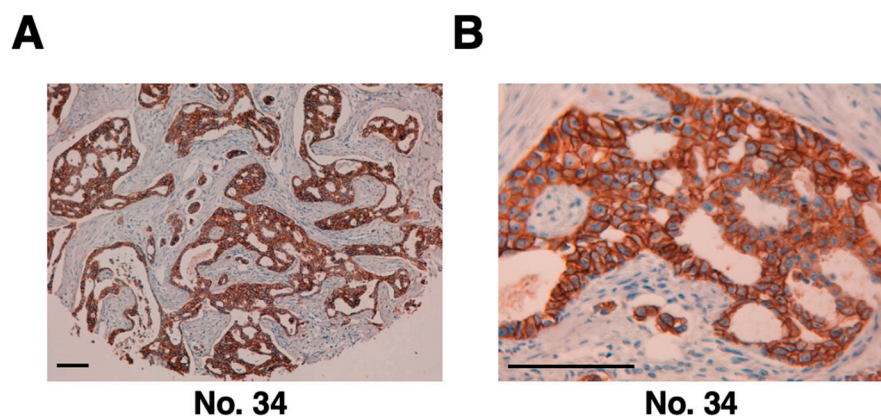


Figure 4. (A,B) Detection of HER2 in breast cancer specimens using immunohistochemical analysis with H₂Mab-77-mG_{2a-f}. Tissue sections from patients with human breast cancer were incubated with

H2Mab-77-mG_{2a-f} at a concentration of 10 µg/mL and then treated with the EnVision+ kit. Scale bar: 100 µm.

Table 1. Immunohistochemical analysis using H2Mab-77-mG_{2a-f} against breast cancer tissue array.

No.	Sex	Age	Pathological Diagnosis	Differentiation	TNM	H2Mab-77-mG _{2a-f}
1	F	44	Invasive ductal carcinoma	Moderately	T2N2M1	-
2	F	58	Medullary carcinoma	Moderately	T2N2M1	-
3	F	40	Invasive ductal carcinoma	Moderately	T2N1M0	2+
4	F	52	Invasive ductal carcinoma	Moderately	T2N2M1	-
5	F	60	Invasive ductal carcinoma	Moderately	T2N1M1	-
6	F	57	Invasive ductal carcinoma	Moderately	T2N0M0	-
7	F	48	Invasive ductal carcinoma	Moderately	T2N0M0	3+
8	F	66	Invasive ductal carcinoma	Moderately	T2N0M0	-
9	F	58	Adenocarcinoma	Moderately	T2N2M1	-
10	F	63	Invasive ductal carcinoma	Moderately	T2N0M0	-
11	F	32	Invasive ductal carcinoma	Moderately	T2N0M0	-
12	F	59	Invasive lobular carcinoma	Well	T2N2M0	-
13	F	44	Invasive lobular carcinoma	Well	T2N2M0	-
14	F	60	Invasive lobular carcinoma	Moderately	T2N1M0	-
15	F	44	Invasive ductal carcinoma	Moderately	T2N2M0	3+
16	F	82	Invasive ductal carcinoma	Moderately	T2N1M1	-
17	F	58	Adenocarcinoma	Moderately	T2N1M1	2+
18	F	57	Invasive ductal carcinoma	Poorly	T3N3M0	-
19	F	41	Invasive ductal carcinoma	Moderately	T2N1M0	-
20	F	44	Invasive ductal carcinoma	Moderately	T2N2M0	1+
21	F	78	Invasive ductal carcinoma	Moderately	T2N1M0	-
22	F	60	Invasive ductal carcinoma	Moderately	T2N0M0	1+
23	F	N/A	Invasive ductal carcinoma	Moderately	T2N1M1	2+
24	F	46	Invasive ductal carcinoma	Moderately	T2N3M1	-
25	F	41	Invasive ductal carcinoma	Moderately	T2N2M0	-
26	F	59	Invasive ductal carcinoma	Poorly	T2N0M0	-
27	F	45	Invasive ductal carcinoma	Poorly	T2N0M0	-
28	F	43	Invasive ductal carcinoma	N/A	T2N1M1	-
29	F	26	Fibroadenoma	N/A	T1N0M0	-
30	F	40	Invasive ductal carcinoma	N/A	T1N0M0	-
31	F	38	Fibroadenoma	N/A	T2N0M0	-
32	F	51	Invasive ductal carcinoma	Moderately	T2N2M0	-
33	F	45	Invasive ductal carcinoma	Poorly	T2N0M0	2+
34	F	45	Invasive ductal carcinoma	Poorly	T2N1M0	3+
35	F	47	Invasive ductal carcinoma	Moderately	T2N1M0	-
36	F	55	Invasive ductal carcinoma	Moderately	T2N3M1	1+
37	F	58	Invasive ductal carcinoma	Moderately	T3N3M0	-
38	F	47	Invasive ductal carcinoma	Moderately	T2N0M0	1+
39	F	38	Invasive ductal carcinoma	Poorly	T2N0M0	-
40	F	40	Invasive ductal carcinoma	Poorly	T2N0M0	-
41	F	57	Invasive ductal carcinoma	Poorly	T2N0M0	-
42	F	42	Invasive ductal carcinoma	Moderately	T2N0M0	3+
43	F	60	Invasive ductal carcinoma	Moderately	T2N0M0	-
44	F	58	Invasive ductal carcinoma	Moderately	T2N0M0	-
45	F	41	Invasive ductal carcinoma	Moderately	T2N0M0	-
46	F	50	Invasive ductal carcinoma	Moderately	T2N0M0	-
47	F	60	Invasive ductal carcinoma	Moderately	T2N2M1	-

48	F	53	Invasive ductal carcinoma	Moderately	T2N0M0	-
49	F	65	Invasive ductal carcinoma	Moderately	T2N0M0	-
50	F	43	Invasive ductal carcinoma	Moderately	T2N0M0	-
51	F	57	Invasive ductal carcinoma	Moderately	T2N0M0	3+
52	F	37	Invasive ductal carcinoma	Moderately	T2N0M0	-
53	F	50	Invasive ductal carcinoma	Moderately	T2N3M0	-
54	F	48	Invasive ductal carcinoma	Poorly	T2N1M0	-
55	F	50	Invasive ductal carcinoma	Moderately	T2N0M0	-
56	F	53	Invasive ductal carcinoma	Moderately	T2N0M0	-
57	F	49	Invasive ductal carcinoma	Moderately	T2N0M0	-
58	F	65	Invasive ductal carcinoma	Moderately	T2N1M0	-
59	F	43	Invasive ductal carcinoma	Moderately	T2N0M0	-
60	F	58	Invasive ductal carcinoma	Moderately	T2N0M0	-
61	F	48	Invasive ductal carcinoma	Moderately	T2N0M0	-
62	F	N/A	Invasive ductal carcinoma	Moderately	N/A	1+
63	F	N/A	Invasive ductal carcinoma	Moderately	N/A	-

N/A, not available; TNM, tumor node metastasis; F, female. -, no stain; 1+, weak intensity; 2+, moderate intensity; 3+, strong intensity

2.5. ADCC and CDC Activities of H₂Mab-77-mG_{2a}-f-Mediated in Breast Cancer

We next tested H₂Mab-77-mG_{2a}-f for ADCC against BT-474 cells (HER2-expressing breast cancer cell line) and MDA-MB-468 cells (HER2-negative breast cancer cell line). As shown in Figure 5A, H₂Mab-77-mG_{2a}-f demonstrated more ADCC (38.9% cytotoxicity) against BT-474 cells than 281-mG_{2a}-f, the control afucosylated mouse IgG_{2a} (5.5% cytotoxicity; $P < 0.001$). In contrast, the ADCC activity of H₂Mab-77-mG_{2a}-f against MDA-MB-468 cells was 9.3% cytotoxicity, which was comparable to that of 281-mG_{2a}-f (10.2% cytotoxicity).

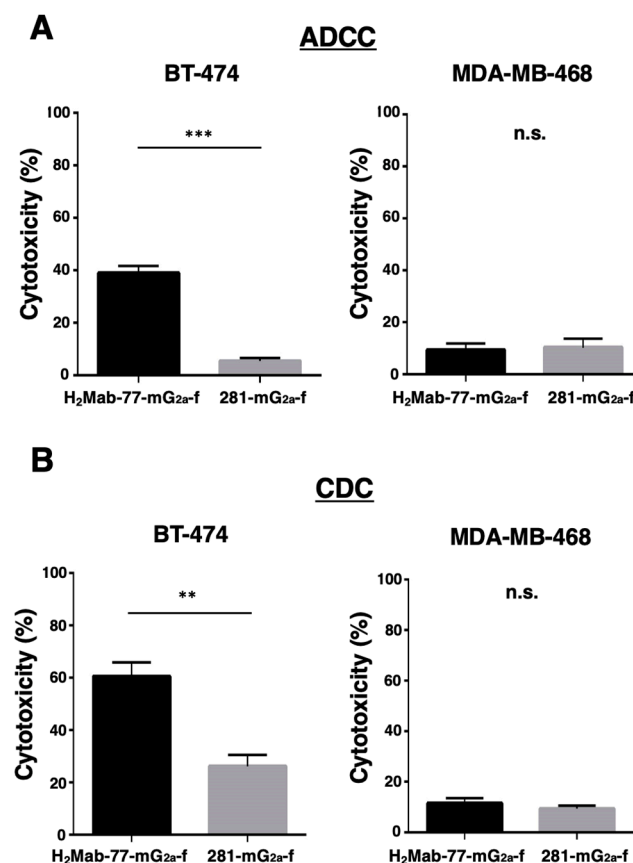


Figure 5. Investigation of the ADCC and CDC activities elicited by H₂Mab-77-mG_{2a-f}. **(A)** Antibody-dependent cellular cytotoxicity (ADCC) elicited by H₂Mab-77-mG_{2a-f} and 281-mG_{2a-f} (control antibodies) targeting BT-474 and MDA-MB-468 cells. **(B)** Complement-dependent cytotoxicity (CDC) elicited by H₂Mab-77-mG_{2a-f} and 281-mG_{2a-f} (control antibodies) targeting BT-474 and MDA-MB-468 cells. Values are presented as the mean ± SEM. Statistical significance is indicated by asterisks (**P < 0.001, *P < 0.01, n.s., not significant, unpaired t-test). ADCC, antibody-dependent cellular cytotoxicity; CDC, complement-dependent cytotoxicity.

Then we looked to see whether H₂Mab-77-mG_{2a-f} had CDC against BT-474 and MDA-MB-468 cells. As indicated in Figure 5B, H₂Mab-77-mG_{2a-f} induced more cytotoxicity (60.5% cytotoxicity) in BT-474 cells than control afucosylated mouse IgG_{2a} (26.1% cytotoxicity; P < 0.01). In contrast, the CDC activity of H₂Mab-77-mG_{2a-f} was 11.4% cytotoxicity against MDA-MB-468 cells, which was comparable to that of 281-mG_{2a-f} (9.3% cytotoxicity). These encouraging findings show that H₂Mab-77-mG_{2a-f} greatly improves both ADCC and CDC activities against HER2-expressing breast cancer cells.

2.6. Antitumor Activities of H₂Mab-77-mG_{2a-f} in the Mouse Xenografts of Breast Tumor Cells

Tumor formation was observed on day 7 in 16 mice inoculated with either BT-474 or MDA-MB-468 cells. The mice bearing breast cancer were divided into two groups: one group received treatment with H₂Mab-77-mG_{2a-f}, and the other group served as the control and received 281-mG_{2a-f}. Intraperitoneal injections of H₂Mab-77-mG_{2a-f} (100 µg) and 281-mG_{2a-f} (100 µg) were administered to the respective groups on days 7, 14, and 21 after cell inoculation. Tumor diameters were measured on days 7, 10, 14, 16, 21, 24, and 28 following cell inoculation. In the BT-474-bearing mice, the group treated with H₂Mab-77-mG_{2a-f} exhibited significantly less tumor growth on days 24 (P < 0.01) and 28 (P < 0.001) compared to the group treated with 281-mG_{2a-f} (Figure 6A). The reduction in tumor volume achieved by H₂Mab-77-mG_{2a-f} treatment was 36.6% on day 28. Conversely, there was no difference in tumor growth between the H₂Mab-77-mG_{2a-f} and 281-mG_{2a-f} treatment groups in the MDA-MB-468-bearing mice (Figure 6B). Additionally, the tumor weight of the BT-474-bearing mice treated with H₂Mab-77-mG_{2a-f} was significantly lower than that of the mice treated with 281-mG_{2a-f} (45.1% reduction; P < 0.01, Figure 6C). However, no difference in tumor weight on day 28 was observed between the H₂Mab-77-mG_{2a-f} and 281-mG_{2a-f} treatment groups in the MDA-MB-468-bearing mice (Figure 6D). Figure 6E,F show the resected tumors from the H₂Mab-77-mG_{2a-f} and 281-mG_{2a-f}-treated groups, respectively, on day 28 after inoculation of BT-474 and MDA-MB-468 cells. There were no significant differences in total body weights between the H₂Mab-77-mG_{2a-f} and 281-mG_{2a-f}-treated groups in both the BT-474 and MDA-MB-468-bearing xenografts (Figure 7A,B). The appearance of mice treated with H₂Mab-77-mG_{2a-f} and 281-mG_{2a-f} on day 28 after cell inoculation is shown in Figure 7C (BT-474) and Figure 7D (MDA-MB-468), respectively. In summary, these results demonstrate the antitumor effects of H₂Mab-77-mG_{2a-f} administration against HER2-positive breast cancer xenografts.

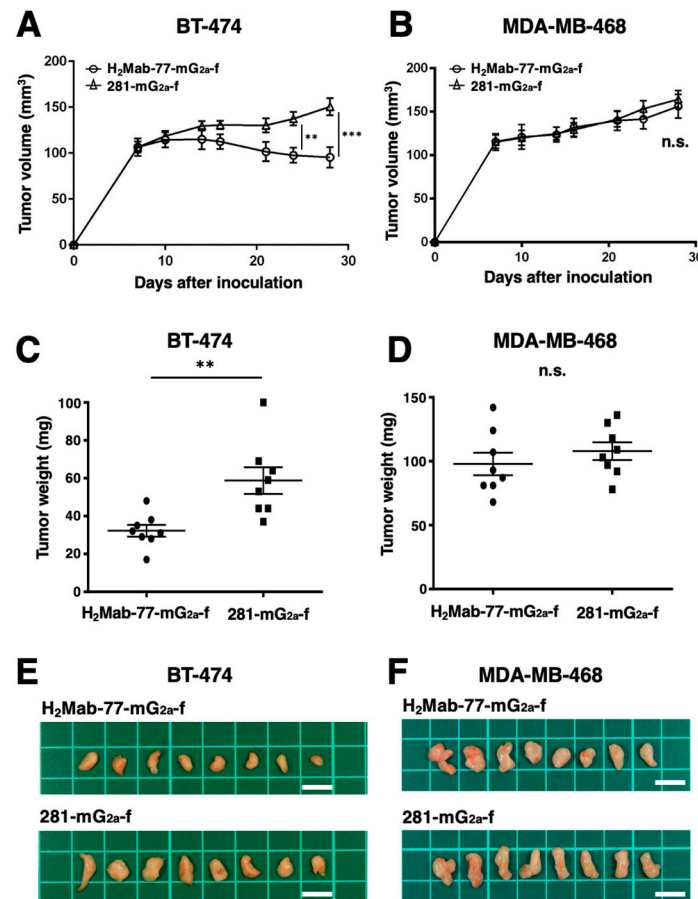


Figure 6. Evaluation of the antitumor activity of H₂Mab-77-mG_{2a}-f in breast cancer xenograft models. (A) BT-474 cells (5×10^6 cells) and (B) MDA-MB-468 cells (5×10^6 cells) were subcutaneously transplanted into the left flanks of mice. On day 7 after transplantation, 100 μ g of H₂Mab-77-mG_{2a}-f and 281-mG_{2a}-f (control) were intraperitoneally injected into mice. Additional antibody treatments were conducted on days 14 and 21. Tumor diameters were measured on days 7, 10, 14, 16, 21, 24, and 28 after the inoculation of tumor cells. Values are presented as the mean \pm SEM. Statistical significance is indicated by asterisks (***P < 0.001, **P < 0.01, n.s., not significant, ANOVA, and Sidak's multiple comparisons test). (C) Tumors of BT-474 and (D) MDA-MB-468 xenografts were resected from H₂Mab-77-mG_{2a}-f and 281-mG_{2a}-f (control) groups. Tumor weight on day 28, tumor weight was measured from the excised xenografts. Values are presented as the mean \pm SEM. Statistical significance is denoted by asterisks (**P < 0.01, n.s., not significant, unpaired t-test). (E) Resected tumors of BT-474 and (F) MDA-MB-468 xenografts from H₂Mab-77-mG_{2a}-f and 281-mG_{2a}-f (control) groups on day 28. Scale bar: 1 cm.

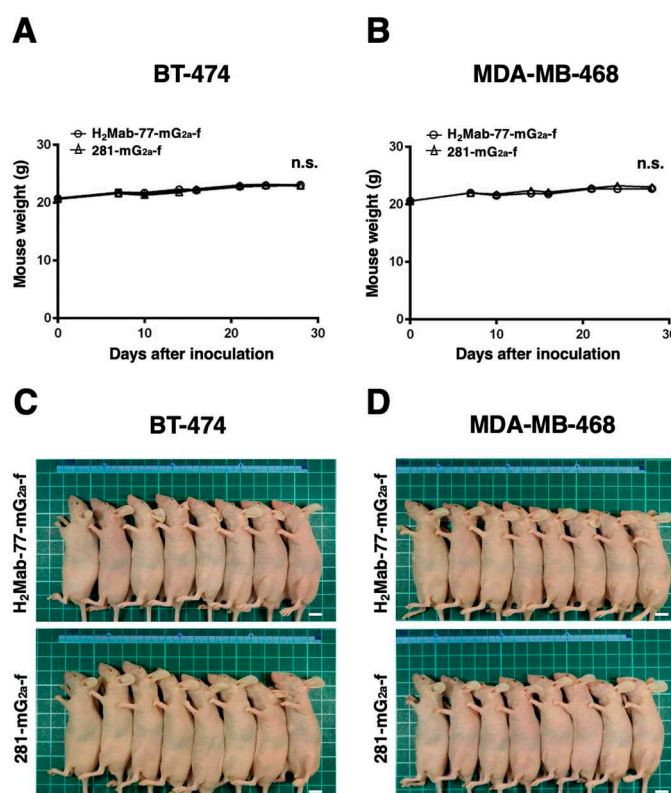


Figure 7. Monitoring the body weights and appearances of mice bearing breast tumor xenografts. (A) Body weights of mice inoculated with BT-474 and (B) MDA-MB-468 xenografts in H₂Mab-77-mG_{2a-f} and 281-mG_{2a-f} (control) groups were recorded on days 7, 10, 14, 16, 21, 24, and 28. Values are mean \pm SEM. No statistical significance is indicated by n.s. (ANOVA and Sidak's multiple comparisons test). (C) Body appearance of BT-474 and (D) MDA-MB-468-implanted mice in H₂Mab-77-mG_{2a-f} and 281-mG_{2a-f} (control) groups on day 28, respectively (scale bar: 1 cm).

3. Discussion

Humanized anti-HER2 mAbs like trastuzumab and pertuzumab have helped patients with HER2-positive breast cancer live longer [23,25,48,49]. Aside from monotherapy with these mAbs, combined treatment with trastuzumab and pertuzumab has been shown to enhance outcomes [50]. The membrane-bound p95 generated by the extracellular cleavage of HER2 by metalloproteinase has kinase activity in HER2-overexpressing cells [31]. The inhibition of this cleavage by trastuzumab may be one of the factors suppressing proliferative signals. Furthermore, the antitumor effects of trastuzumab is probably mediated by indirect mechanisms such as ADCC activity [44]. In the future, we will look into the impacts of H₂Mab-77-mG_{2a-f} on dimer formation and HER2 shedding to better understand the mechanism of the antitumor action by H₂Mab-77-mG_{2a-f}.

The development of significant acquired resistance is a challenge for the therapeutic use of trastuzumab [51,52]. Concerns have been raised that even strong ADCs, such as T-DM1, may develop resistance owing to diminished antigen binding, poor internalization, lysosomal degradation errors, and accelerated cellular drug clearance by drug-efflux pumps [53]. MUC4, a membrane-associated mucin known to mask membrane proteins, has been shown to inhibit trastuzumab binding to HER2 [54]. Furthermore, MUC4 acts as an intramembranous ligand and activator of HER2, resulting in the inhibition of apoptosis in cancer cells [55].

Antibodies have distinct activities depending on their binding epitopes, similar to trastuzumab and pertuzumab. The FDA-approved margetuximab and trastuzumab have comparable epitopes and binding affinity; however, margetuximab has a greater binding capacity to the ADCC activator Fc γ RIIIa and a lower affinity for the immune activation inhibitor CD32B [56–58]. Patients with breast cancer who have low-binding Fc γ RIIIa alleles may also benefit from a combination of margetuximab

and anti-HER2 treatments [59]. When used in conjunction with trastuzumab, the HER2-targeted humanized mAb 1E11 inhibits the growth of HER2-expressing gastric tumors by binding to the HER2 domain IV, which does not overlap with trastuzumab [60]. Therefore, one of the primary strategies for combating drug resistance is the development of antibodies with a variety of features, including the binding epitope. H₂Mab-19, H₂Mab-41, H₂Mab-77, H₂Mab-119, H₂Mab-139, and H₂Mab-181 are anti-HER2 mAbs that we have previously established and proven to have antitumor effects [43,61–66]. In our early findings, these mAbs have different epitopes, including the HER2 domains I, III, and IV. Trastuzumab and anti-HER2 antibodies that target several epitopes actually have a stronger antitumor impact than standalone therapies [37].

The modified H₂Mab-77-mG_{2a}-f demonstrated ADCC and CDC activities depending on HER2 expression as well as superior antitumor effects in xenograft models of HER2-positive breast cancer (Figures 5 and 6). Combining H₂Mab-77-mG_{2a}-f with other HER2-targeted medicines has the potential to overcome resistance to HER2 antibody therapy. HER2-positive breast tumors account for around half of all brain metastases [19,67,68]. In a future investigation, we will confirm the inhibitory impact of H₂Mab-77-mG_{2a}-f on this metastasis.

Bispecific antibodies targeting HER2×CD3 (ertumaxomab), HER2×CD16, and HER2×HER3 (zenocutuzumab: MCLA-128 and MM-111) are being developed in addition to naive antibodies [69–74]. Recently, progress has been made in the creation of bispecific antibodies that target both the immune checkpoint molecules PD-1/PD-L1 and HER2, with antitumor effects proven in preclinical animals [75,76]. In trastuzumab-resistant cancer models, bispecific antibodies targeting immune checkpoint molecules and HER2 may be more successful than individual mAb treatments. The use of H₂Mabs to create bispecific antibodies is another option for increasing anti-HER2 treatment. Furthermore, attention has been drawn to chimeric antigen receptor-T (CAR-T) cell treatment, which possesses both antibody specificity and T cell cytotoxicity [77–79]. While the FDA authorized the first CD19 CAR-T treatment for B-cell lymphoma in 2017, no CAR-T therapeutic targeting HER2 has yet to be produced [80]. In preclinical settings, we previously showed that anti-podoplanin CAR-T cells, in which we incorporated the created anti-podoplanin mAb into T cells, had strong antitumor efficacy and may release proinflammatory cytokines [81,82]. The future possibilities of H₂Mab-77 for HER2-targeting CAR-T applications are hoped for.

4. Materials and Methods

4.1. Cell Lines

Human breast cancer cell lines (BT-474 and MDA-MB-468) and a human glioblastoma cell line (LN229) were obtained from the American Type Culture Collection (Manassas, VA). To establish a HER2-overexpressed LN229 cell line (LN229/HER2), LN229 cells were transfected with the pCAG/HER2-RAPMAP plasmid using the Neon Transfection System (Thermo Fisher Scientific, Inc., Waltham, MA), as previously [43,83,84] described. All cells were cultured in Dulbecco's modified Eagle's medium (DMEM; Nacalai Tesque, Inc., Kyoto, Japan) supplemented with 10% heat-inactivated fetal bovine serum (FBS; Thermo Fisher Scientific, Inc.), 100 µg/mL streptomycin, 100 units/ml penicillin, and 0.25 µg/mL amphotericin B (Nacalai Tesque, Inc.). The cells were maintained in a humidified incubator at 37°C with 5% CO₂ and 95% air atmosphere.

4.2. Animals

To reduce animal hardship and suffering, all animal studies were carried out in compliance with the rules and recommendations. The Institutional Committee for Experiments of the Institute of Microbial Chemistry (Numazu, Japan) authorized animal studies for H₂Mab-77-mG_{2a}-f's antitumor efficacy (approval numbers 2023-001 and 2023-018). Over the course of the trial, mice were kept in a specified pathogen-free environment on an 11 h light/13 h dark cycle with access to food and drink as needed. Throughout the course of the trials, mice were frequently checked for weight and health conditions every two to five days. Humane objectives for euthanasia were established as a loss of original body weight to a point >25% and/or a maximal tumor size >3,000 mm³.

4.3. Antibodies

H₂Mab-77, an anti-HER2 mAb, was developed as previously mentioned [43]. We cloned the V_H cDNA of H₂Mab-77 and the C_H of mouse IgG_{2a} into the pCAG-Ble vector (FUJIFILM Wako Pure Chemical Corporation, Osaka, Japan) in order to change the subclass of H₂Mab-77 from mouse IgG₁ to mouse IgG_{2a} (H₂Mab-77-mG_{2a}). Additionally, the pCAG-Neo vector (FUJIFILM Wako Pure Chemical Corporation) was used to clone the V_L cDNA of H₂Mab-77 and the C_L cDNA of the mouse kappa light chain. Using the ExpiCHO Expression System from Thermo Fisher Scientific, Inc., the vector for H₂Mab-77-mG_{2a} was transfected into BINDS-09, FUT8-knockout ExpiCHO-S cells. Using Ab-Capcher (ProteNova Co., Ltd., Kanagawa, Japan), H₂Mab-77-mG_{2a}-f, an afucosylated variant of the original antibody, was isolated. For the evaluation of western blotting, RcMab-1, an anti-isocitrate dehydrogenase 1 [IDH1] mAb, was utilized as an internal control. For the investigation of ADCC, CDC, and *in vivo* antitumor effectiveness, 281-mG_{2a}-f (an afucosylated anti-hamster podoplanin mAb) was employed as an afucosylated reference mouse IgG_{2a} [85–87].

4.4. Flow Cytometry

Cells were harvested using 0.25% trypsin and 1 mM ethylenediaminetetraacetic acid (EDTA; Nacalai Tesque, Inc.). Subsequently, they were washed with 0.1% bovine serum albumin (Nacalai Tesque, Inc.) in phosphate-buffered saline (PBS), followed by treatment with H₂Mab-77-mG_{2a}-f (1 or 10 µg/mL) for 30 minutes at 4°C. Then, cells were incubated with Alexa Fluor 488-conjugated anti-mouse IgG (1:2000 dilution; Cell Signaling Technology, Inc., Danvers, MA), and fluorescence was measured using an SA3800 Cell Analyzer (Sony Corp., Tokyo, Japan).

4.5. Determination of the Binding Affinity by Flow Cytometry

After being suspended in 100 µL of serially diluted H₂Mab-77-mG_{2a}-f (0.0006–10 µg/mL), the cells were then incubated with 1:200 of Cell Signaling Technology, Inc.'s Alexa Fluor 488-conjugated anti-mouse IgG. The SA3800 Cell Analyzer (Sony Corp.) flow cytometer was then used to gather fluorescence data. The binding isotherms were fitted into the built-in, one-site binding model in GraphPad PRISM 6 (GraphPad Software, Inc., La Jolla, CA) to calculate the dissociation constant (*K_D*).

4.6. Western Blotting

Cell pellets were resuspended in phosphate-buffered saline (PBS; Nacalai Tesque, Inc.) containing 1% Triton X-100 (FUJIFILM Wako Pure Chemical Corp.) and 50 µg/mL aprotinin (Nacalai Tesque, Inc.). Cell debris was removed by centrifugation at 21,880 × g for 10 minutes at 4°C. Protein concentration was determined using the bicinchoninic acid (BCA) method. Cell lysates (10 µg) were boiled in sodium dodecyl sulfate sample buffer (Nacalai Tesque, Inc.). Proteins were separated on 5–20% polyacrylamide gels (FUJIFILM Wako Pure Chemical Corp.) and transferred onto polyvinylidene difluoride (PVDF) membranes (Merck KGaA). PVDF membranes were blocked with 4% skim milk (Nacalai Tesque, Inc.) for 30 minutes at room temperature. The membranes were then incubated with H₂Mab-77-mG_{2a}-f (1 µg/mL) and RcMab-1 (1 µg/mL) for additional 30 minutes at room temperature. Subsequently, the membranes were incubated with peroxidase-conjugated anti-mouse immunoglobulins (diluted 1:2000; Agilent Technologies, Inc., Santa Clara, CA) and peroxidase-conjugated anti-rat immunoglobulins (diluted 1:10000; Sigma-Aldrich Corp.) for 30 minutes. Blots were developed using ImmunoStar LD (FUJIFILM Wako Pure Chemical Corp.) or Pierce™ ECL Plus Western Blotting Substrate (Thermo Fisher Scientific, Inc.) and imaged with a Sayaca-Imager (DRC Co., Ltd., Tokyo, Japan). Image analysis was performed using Qcapture Pro software (DRC Co., Ltd.).

4.7. Immunohistochemical Analysis

After being autoclaved in EnVision FLEX Target Retrieval Solution High pH (Agilent Technologies, Inc.) for 20 min, paraffin-embedded tissue sections from the breast cancer tissue array (Cat. No. T8235721-5, Lot. No. B904111; BioChain, San Francisco, CA, USA) were treated with 3% hydrogen peroxide for 15 minutes at room temperature. Thermo Fisher Scientific, Inc.'s SuperBlock

T20 was used to block the tissue sections before H₂Mab-77-mG_{2a-f} (10 µg/mL) and the EnVision+ Kit for mice (Agilent Technologies, Inc.) were applied for 60 minutes at room temperature each. 3,3'-diaminobenzidine tetrahydrochloride (DAB; Agilent Technologies, Inc.) was used to create the color for 2 minutes at room temperature. Mayer's hematoxylin solution (FUJIFILM Wako Pure Chemical Corporation) was used for counterstaining. The sections were examined using Leica DMD108 (Leica Microsystems GmbH, Wetzlar, Germany) to capture pictures.

4.8. ADCC of H₂Mab-77-mG_{2a-f}

The following evaluation was made of H₂Mab-77-mG_{2a-f}'s ability to induce ADCC. Five-week-old female BALB/c nude mice were bought from Charles River Laboratories, Inc. Splens were extracted aseptically after cervical dislocation euthanasia. Spleen tissues were then processed through a sterile cell strainer (352360, BD Falcon) using a syringe to produce single-cell suspensions. A 10-second exposure to ice-cold, distilled water destroyed erythrocytes. Effector cells were created by resuspending the splenocytes in DMEM with 10% FBS after being cleaned with DMEM. Thermo Fisher Scientific, Inc.'s 10 µg/mL Calcein AM was used to mark the target cells (BT-474 and MDA-MB-468) for the study. In 96-well plates, target cells (2 × 10⁴ cells) were seeded before effector cells (effector to target ratio, 50:1) and 100 µg/mL of either H₂Mab-77-mG_{2a-f} or 281-mG_{2a-f} were added. A microplate reader (Power Scan HT; BioTek Instruments, Inc.) with an excitation wavelength of 485 nm and an emission wavelength of 538 nm was used to analyze the Calcein release into the medium after a 4.5-hour incubation at 37°C.

This is how cytotoxicity (% lysis) was determined: % lysis is calculated as $(E - S)/(M - S) \times 100$, where "E" denotes the fluorescence in effector and target cell cultures, "S" denotes the spontaneous fluorescence of only target cells, and "M" denotes the maximum fluorescence after treatment with a lysis buffer (10 mM Tris-HCl (pH 7.4), 10 mM EDTA, and 0.5% Triton X-100). The Institutional Committee for trials of the Institute of Microbial Chemistry (Numazu, Japan) authorized animal trials for ADCC of H₂Mab-77-mG_{2a-f} (permission number 2023-018).

4.9. CDC of H₂Mab-77-mG_{2a-f}

The following procedure was used to assess how well H₂Mab-77-mG_{2a-f} induced CDC. With 10 µg/mL Calcein AM, the target cells (BT-474 and MDA-MB-468) were marked. Target cells (2 × 10⁴ cells) were put in 96-well plates with 100 µg/mL of either H₂Mab-77-mG_{2a-f} or 281-mG_{2a-f} and rabbit complement (final dilution 1:10; Low-Tox-M Rabbit Complement; Cedarlane Laboratories). The amount of calcein released into the medium was measured during 4.5-hour incubation at 37°C.

4.10. Antitumor Activities of H₂Mab-77-mG_{2a-f} in Xenografts of Breast Cancer

Charles River Laboratories, Inc. provided the BALB/c nude mice (female, 5 weeks old). Cells from BT-474 and MDA-MB-468 were mixed with DMEM and BD Biosciences' Matrigel Matrix Growth Factor Reduced. Subcutaneous injections were then given to the mice's left flanks. On the seventh post-inoculation day, 100 µg of H₂Mab-77-mG_{2a-f} (n = 8) or 281-mG_{2a-f} (n = 8) in 100 µL PBS were administered intraperitoneally. Additional antibody injections were given on days 14 and 21. The tumor diameter was assessed on days 7, 10, 14, 16, 21, 24, and 28 after breast cancer cell implantation. Tumor volumes were calculated in the same manner as previously stated. The weight of the mice was also assessed on days 7, 10, 14, 16, 21, 24, and 28 following breast cancer cell inoculation. When the observations were finished on day 28, the mice were killed, and tumor weights were assessed following tumor excision.

Author Contributions: T.T., H.S., and T.O. performed the experiments. M.K.K. and Y.K. designed the experiments. T.T. and H.S. analyzed the data and wrote the manuscript. All authors have read and agreed to the manuscript.

Funding: This research was supported in part by Japan Agency for Medical Research and Development (AMED) under Grant Numbers: JP23ama121008 (Y.K.), JP23am0401013 (Y.K.), and JP23ck0106730 (Y.K.).

Institutional Review Board Statement: Animal experiments were approved by the Institutional Committee for Experiments of the Institute of Microbial Chemistry (approval no. 2022-056, 2023-001, and 2023-018).

Informed Consent Statement: Not applicable.

Data Availability Statement: The data presented in this study are available in the article and supplementary material.

Conflicts of Interest: The authors have no conflicts of interest to declare.

References

1. Pal, S.K.; Pegram, M. Targeting HER2 Epitopes. *Semin Oncol* **2006**, *33*, 386-391, doi:10.1053/j.seminoncol.2006.04.004.
2. Agus, D.B.; Akita, R.W.; Fox, W.D.; Lewis, G.D.; Higgins, B.; Pisacane, P.I.; Lofgren, J.A.; Tindell, C.; Evans, D.P.; Maiese, K.; et al. Targeting ligand-activated ErbB2 signaling inhibits breast and prostate tumor growth. *Cancer Cell* **2002**, *2*, 127-137, doi:10.1016/s1535-6108(02)00097-1.
3. Garrett, T.P.; McKern, N.M.; Lou, M.; Elleman, T.C.; Adams, T.E.; Lovrecz, G.O.; Kofler, M.; Jorissen, R.N.; Nice, E.C.; Burgess, A.W.; et al. The crystal structure of a truncated ErbB2 ectodomain reveals an active conformation, poised to interact with other ErbB receptors. *Mol Cell* **2003**, *11*, 495-505, doi:10.1016/s1097-2765(03)00048-0.
4. Wallasch, C.; Weiss, F.U.; Niederfellner, G.; Jallal, B.; Issing, W.; Ullrich, A. Heregulin-dependent regulation of HER2/neu oncogenic signaling by heterodimerization with HER3. *Embo j* **1995**, *14*, 4267-4275, doi:10.1002/j.1460-2075.1995.tb00101.x.
5. Alimandi, M.; Romano, A.; Curia, M.C.; Muraro, R.; Fedi, P.; Aaronson, S.A.; Di Fiore, P.P.; Kraus, M.H. Cooperative signaling of ErbB3 and ErbB2 in neoplastic transformation and human mammary carcinomas. *Oncogene* **1995**, *10*, 1813-1821.
6. Pinkas-Kramarski, R.; Soussan, L.; Waterman, H.; Levkowitz, G.; Alroy, I.; Klapper, L.; Lavi, S.; Seger, R.; Ratzkin, B.J.; Sela, M.; et al. Diversification of Neu differentiation factor and epidermal growth factor signaling by combinatorial receptor interactions. *Embo j* **1996**, *15*, 2452-2467.
7. Siegel, R.L.; Miller, K.D.; Wagle, N.S.; Jemal, A. Cancer statistics, 2023. *CA Cancer J Clin* **2023**, *73*, 17-48, doi:10.3322/caac.21763.
8. Cronin, K.A.; Harlan, L.C.; Dodd, K.W.; Abrams, J.S.; Ballard-Barbash, R. Population-based estimate of the prevalence of HER-2 positive breast cancer tumors for early stage patients in the US. *Cancer Invest* **2010**, *28*, 963-968, doi:10.3109/07357907.2010.496759.
9. Guarneri, V.; Barbieri, E.; Dieci, M.V.; Piacentini, F.; Conte, P. Anti-HER2 neoadjuvant and adjuvant therapies in HER2 positive breast cancer. *Cancer Treat Rev* **2010**, *36 Suppl 3*, S62-66, doi:10.1016/s0305-7372(10)70022-0.
10. Abd El-Rehim, D.M.; Pinder, S.E.; Paish, C.E.; Bell, J.A.; Rampaul, R.S.; Blamey, R.W.; Robertson, J.F.; Nicholson, R.I.; Ellis, I.O. Expression and co-expression of the members of the epidermal growth factor receptor (EGFR) family in invasive breast carcinoma. *Br J Cancer* **2004**, *91*, 1532-1542, doi:10.1038/sj.bjc.6602184.
11. Purdie, C.A.; Baker, L.; Ashfield, A.; Chatterjee, S.; Jordan, L.B.; Quinlan, P.; Adamson, D.J.; Dewar, J.A.; Thompson, A.M. Increased mortality in HER2 positive, oestrogen receptor positive invasive breast cancer: a population-based study. *Br J Cancer* **2010**, *103*, 475-481, doi:10.1038/sj.bjc.6605799.
12. Herter-Sprie, G.S.; Greulich, H.; Wong, K.K. Activating Mutations in ERBB2 and Their Impact on Diagnostics and Treatment. *Front Oncol* **2013**, *3*, 86, doi:10.3389/fonc.2013.00086.
13. Slamon, D.J.; Clark, G.M.; Wong, S.G.; Levin, W.J.; Ullrich, A.; McGuire, W.L. Human breast cancer: correlation of relapse and survival with amplification of the HER-2/neu oncogene. *Science* **1987**, *235*, 177-182, doi:10.1126/science.3798106.
14. Puglisi, F.; Fontanella, C.; Amoroso, V.; Bianchi, G.V.; Bisagni, G.; Falci, C.; Fontana, A.; Generali, D.; Gianni, L.; Grassadonia, A.; et al. Current challenges in HER2-positive breast cancer. *Crit Rev Oncol Hematol* **2016**, *98*, 211-221, doi:10.1016/j.critrevonc.2015.10.016.
15. Hayes, D.F. HER2 and Breast Cancer - A Phenomenal Success Story. *N Engl J Med* **2019**, *381*, 1284-1286, doi:10.1056/NEJMcibr1909386.
16. Arteaga, C.L.; Engelman, J.A. ERBB receptors: from oncogene discovery to basic science to mechanism-based cancer therapeutics. *Cancer Cell* **2014**, *25*, 282-303, doi:10.1016/j.ccr.2014.02.025.

17. Riecke, K.; Witzel, I. Targeting the Human Epidermal Growth Factor Receptor Family in Breast Cancer beyond HER2. *Breast Care (Basel)* **2020**, *15*, 579-585, doi:10.1159/000510998.
18. Martin, A.M.; Cagney, D.N.; Catalano, P.J.; Warren, L.E.; Bellon, J.R.; Punglia, R.S.; Claus, E.B.; Lee, E.Q.; Wen, P.Y.; Haas-Kogan, D.A.; et al. Brain Metastases in Newly Diagnosed Breast Cancer: A Population-Based Study. *JAMA Oncol* **2017**, *3*, 1069-1077, doi:10.1001/jamaoncol.2017.0001.
19. Kuksis, M.; Gao, Y.; Tran, W.; Hoey, C.; Kiss, A.; Komorowski, A.S.; Dhaliwal, A.J.; Sahgal, A.; Das, S.; Chan, K.K.; et al. The incidence of brain metastases among patients with metastatic breast cancer: a systematic review and meta-analysis. *Neuro Oncol* **2021**, *23*, 894-904, doi:10.1093/neuonc/noaa285.
20. Wolff, A.C.; Hammond, M.E.; Schwartz, J.N.; Hagerty, K.L.; Allred, D.C.; Cote, R.J.; Dowsett, M.; Fitzgibbons, P.L.; Hanna, W.M.; Langer, A.; et al. American Society of Clinical Oncology/College of American Pathologists guideline recommendations for human epidermal growth factor receptor 2 testing in breast cancer. *J Clin Oncol* **2007**, *25*, 118-145, doi:10.1200/jco.2006.09.2775.
21. Ross, J.S.; Slodkowska, E.A.; Symmans, W.F.; Pusztai, L.; Ravdin, P.M.; Hortobagyi, G.N. The HER-2 receptor and breast cancer: ten years of targeted anti-HER-2 therapy and personalized medicine. *Oncologist* **2009**, *14*, 320-368, doi:10.1634/theoncologist.2008-0230.
22. Cobleigh, M.A.; Vogel, C.L.; Tripathy, D.; Robert, N.J.; Scholl, S.; Fehrenbacher, L.; Wolter, J.M.; Paton, V.; Shak, S.; Lieberman, G.; et al. Multinational study of the efficacy and safety of humanized anti-HER2 monoclonal antibody in women who have HER2-overexpressing metastatic breast cancer that has progressed after chemotherapy for metastatic disease. *J Clin Oncol* **1999**, *17*, 2639-2648, doi:10.1200/jco.1999.17.9.2639.
23. Slamon, D.J.; Leyland-Jones, B.; Shak, S.; Fuchs, H.; Paton, V.; Bajamonde, A.; Fleming, T.; Eiermann, W.; Wolter, J.; Pegram, M.; et al. Use of chemotherapy plus a monoclonal antibody against HER2 for metastatic breast cancer that overexpresses HER2. *N Engl J Med* **2001**, *344*, 783-792, doi:10.1056/nejm200103153441101.
24. Vogel, C.L.; Cobleigh, M.A.; Tripathy, D.; Gutheil, J.C.; Harris, L.N.; Fehrenbacher, L.; Slamon, D.J.; Murphy, M.; Novotny, W.F.; Burchmore, M.; et al. Efficacy and safety of trastuzumab as a single agent in first-line treatment of HER2-overexpressing metastatic breast cancer. *J Clin Oncol* **2002**, *20*, 719-726, doi:10.1200/jco.2002.20.3.719.
25. Amiri-Kordestani, L.; Blumenthal, G.M.; Xu, Q.C.; Zhang, L.; Tang, S.W.; Ha, L.; Weinberg, W.C.; Chi, B.; Candau-Chacon, R.; Hughes, P.; et al. FDA approval: ado-trastuzumab emtansine for the treatment of patients with HER2-positive metastatic breast cancer. *Clin Cancer Res* **2014**, *20*, 4436-4441, doi:10.1158/1078-0432.Ccr-14-0012.
26. Nakada, T.; Sugihara, K.; Jikoh, T.; Abe, Y.; Agatsuma, T. The Latest Research and Development into the Antibody-Drug Conjugate, [fam-] Trastuzumab Deruxtecan (DS-8201a), for HER2 Cancer Therapy. *Chem Pharm Bull (Tokyo)* **2019**, *67*, 173-185, doi:10.1248/cpb.c18-00744.
27. Zheng, Y.; Zou, J.; Sun, C.; Peng, F.; Peng, C. Ado-trastuzumab emtansine beyond breast cancer: therapeutic role of targeting other HER2-positive cancers. *Front Mol Biosci* **2023**, *10*, 1165781, doi:10.3389/fmolb.2023.1165781.
28. Hudis, C.A. Trastuzumab--mechanism of action and use in clinical practice. *N Engl J Med* **2007**, *357*, 39-51, doi:10.1056/NEJMra043186.
29. Cho, H.S.; Mason, K.; Ramyar, K.X.; Stanley, A.M.; Gabelli, S.B.; Denney, D.W., Jr.; Leahy, D.J. Structure of the extracellular region of HER2 alone and in complex with the Herceptin Fab. *Nature* **2003**, *421*, 756-760, doi:10.1038/nature01392.
30. Shi, Y.; Fan, X.; Deng, H.; Brezski, R.J.; Ryczyn, M.; Jordan, R.E.; Strohl, W.R.; Zou, Q.; Zhang, N.; An, Z. Trastuzumab triggers phagocytic killing of high HER2 cancer cells in vitro and in vivo by interaction with Fcγ receptors on macrophages. *J Immunol* **2015**, *194*, 4379-4386, doi:10.4049/jimmunol.1402891.
31. Molina, M.A.; Codony-Servat, J.; Albanell, J.; Rojo, F.; Arribas, J.; Baselga, J. Trastuzumab (herceptin), a humanized anti-Her2 receptor monoclonal antibody, inhibits basal and activated Her2 ectodomain cleavage in breast cancer cells. *Cancer Res* **2001**, *61*, 4744-4749.
32. Loo, L.; Capobianco, J.A.; Wu, W.; Gao, X.; Shih, W.Y.; Shih, W.H.; Pourrezaei, K.; Robinson, M.K.; Adams, G.P. Highly sensitive detection of HER2 extracellular domain in the serum of breast cancer patients by piezoelectric microcantilevers. *Anal Chem* **2011**, *83*, 3392-3397, doi:10.1021/ac103301r.
33. Junttila, T.T.; Li, G.; Parsons, K.; Phillips, G.L.; Sliwkowski, M.X. Trastuzumab-DM1 (T-DM1) retains all the mechanisms of action of trastuzumab and efficiently inhibits growth of lapatinib insensitive breast cancer. *Breast Cancer Res Treat* **2011**, *128*, 347-356, doi:10.1007/s10549-010-1090-x.

34. Ogitani, Y.; Hagihara, K.; Oitate, M.; Naito, H.; Agatsuma, T. Bystander killing effect of DS-8201a, a novel anti-human epidermal growth factor receptor 2 antibody-drug conjugate, in tumors with human epidermal growth factor receptor 2 heterogeneity. *Cancer Sci* **2016**, *107*, 1039-1046, doi:10.1111/cas.12966.
35. Li, B.T.; Smit, E.F.; Goto, Y.; Nakagawa, K.; Udagawa, H.; Mazières, J.; Nagasaka, M.; Bazhenova, L.; Saltos, A.N.; Felip, E.; et al. Trastuzumab Deruxtecan in HER2-Mutant Non-Small-Cell Lung Cancer. *N Engl J Med* **2022**, *386*, 241-251, doi:10.1056/NEJMoa2112431.
36. Shitara, K.; Bang, Y.J.; Iwasa, S.; Sugimoto, N.; Ryu, M.H.; Sakai, D.; Chung, H.C.; Kawakami, H.; Yabusaki, H.; Lee, J.; et al. Trastuzumab Deruxtecan in Previously Treated HER2-Positive Gastric Cancer. *N Engl J Med* **2020**, *382*, 2419-2430, doi:10.1056/NEJMoa2004413.
37. Spiridon, C.I.; Ghetie, M.A.; Uhr, J.; Marches, R.; Li, J.L.; Shen, G.L.; Vitetta, E.S. Targeting multiple Her-2 epitopes with monoclonal antibodies results in improved antigrowth activity of a human breast cancer cell line in vitro and in vivo. *Clin Cancer Res* **2002**, *8*, 1720-1730.
38. Harbeck, N.; Beckmann, M.W.; Rody, A.; Schneeweiss, A.; Müller, V.; Fehm, T.; Marschner, N.; Gluz, O.; Schrader, I.; Heinrich, G.; et al. HER2 Dimerization Inhibitor Pertuzumab - Mode of Action and Clinical Data in Breast Cancer. *Breast Care (Basel)* **2013**, *8*, 49-55, doi:10.1159/000346837.
39. Barthélémy, P.; Leblanc, J.; Goldbarg, V.; Wendling, F.; Kurtz, J.E. Pertuzumab: development beyond breast cancer. *Anticancer Res* **2014**, *34*, 1483-1491.
40. Franklin, M.C.; Carey, K.D.; Vajdos, F.F.; Leahy, D.J.; de Vos, A.M.; Sliwkowski, M.X. Insights into ErbB signaling from the structure of the ErbB2-pertuzumab complex. *Cancer Cell* **2004**, *5*, 317-328, doi:10.1016/s1535-6108(04)00083-2.
41. Clynes, R.A.; Towers, T.L.; Presta, L.G.; Ravetch, J.V. Inhibitory Fc receptors modulate in vivo cytotoxicity against tumor targets. *Nat Med* **2000**, *6*, 443-446, doi:10.1038/74704.
42. Hou, Y.; Nitta, H.; Li, Z. HER2 Intratumoral Heterogeneity in Breast Cancer, an Evolving Concept. *Cancers (Basel)* **2023**, *15*, doi:10.3390/cancers15102664.
43. Itai, S.; Fujii, Y.; Kaneko, M.K.; Yamada, S.; Nakamura, T.; Yanaka, M.; Saidoh, N.; Chang, Y.W.; Handa, S.; Takahashi, M.; et al. H2Mab-77 is a Sensitive and Specific Anti-HER2 Monoclonal Antibody Against Breast Cancer. *Monoclon Antib Immunodiagn Immunother* **2017**, *36*, 143-148, doi:10.1089/mab.2017.0026.
44. Tsao, L.C.; Force, J.; Hartman, Z.C. Mechanisms of Therapeutic Antitumor Monoclonal Antibodies. *Cancer Res* **2021**, *81*, 4641-4651, doi:10.1158/0008-5472.Can-21-1109.
45. Shinkawa, T.; Nakamura, K.; Yamane, N.; Shoji-Hosaka, E.; Kanda, Y.; Sakurada, M.; Uchida, K.; Anazawa, H.; Satoh, M.; Yamasaki, M.; et al. The absence of fucose but not the presence of galactose or bisecting N-acetylglucosamine of human IgG1 complex-type oligosaccharides shows the critical role of enhancing antibody-dependent cellular cytotoxicity. *J Biol Chem* **2003**, *278*, 3466-3473, doi:10.1074/jbc.M210665200.
46. Kaneko, M.K.; Ohishi, T.; Nakamura, T.; Inoue, H.; Takei, J.; Sano, M.; Asano, T.; Sayama, Y.; Hosono, H.; Suzuki, H.; et al. Development of Core-Fucose-Deficient Humanized and Chimeric Anti-Human Podoplanin Antibodies. *Monoclon Antib Immunodiagn Immunother* **2020**, *39*, 167-174, doi:10.1089/mab.2020.0019.
47. Song, K.H.; Trudeau, T.; Kar, A.; Borden, M.A.; Gutierrez-Hartmann, A. Ultrasound-mediated delivery of siESE complexed with microbubbles attenuates HER2+/- cell line proliferation and tumor growth in rodent models of breast cancer. *Nanotheranostics* **2019**, *3*, 212-222, doi:10.7150/ntno.31827.
48. Valabrega, G.; Montemurro, F.; Aglietta, M. Trastuzumab: mechanism of action, resistance and future perspectives in HER2-overexpressing breast cancer. *Ann Oncol* **2007**, *18*, 977-984, doi:10.1093/annonc/mdl475.
49. Amiri-Kordestani, L.; Wedam, S.; Zhang, L.; Tang, S.; Tilley, A.; Ibrahim, A.; Justice, R.; Pazdur, R.; Cortazar, P. First FDA approval of neoadjuvant therapy for breast cancer: pertuzumab for the treatment of patients with HER2-positive breast cancer. *Clin Cancer Res* **2014**, *20*, 5359-5364, doi:10.1158/1078-0432.Ccr-14-1268.
50. Swain, S.M.; Kim, S.B.; Cortés, J.; Ro, J.; Semiglazov, V.; Campone, M.; Ciruelos, E.; Ferrero, J.M.; Schneeweiss, A.; Knott, A.; et al. Pertuzumab, trastuzumab, and docetaxel for HER2-positive metastatic breast cancer (CLEOPATRA study): overall survival results from a randomised, double-blind, placebo-controlled, phase 3 study. *Lancet Oncol* **2013**, *14*, 461-471, doi:10.1016/s1470-2045(13)70130-x.
51. Derakhshani, A.; Rezaei, Z.; Safarpour, H.; Sabri, M.; Mir, A.; Sanati, M.A.; Vahidian, F.; Gholamiyan Moghadam, A.; Aghadokht, A.; Hajiasgharzadeh, K.; et al. Overcoming trastuzumab resistance in HER2-positive breast cancer using combination therapy. *J Cell Physiol* **2020**, *235*, 3142-3156, doi:10.1002/jcp.29216.

52. Vivekanandhan, S.; Knutson, K.L. Resistance to Trastuzumab. *Cancers (Basel)* **2022**, *14*, doi:10.3390/cancers14205115.
53. Khoury, R.; Saleh, K.; Khalife, N.; Saleh, M.; Chahine, C.; Ibrahim, R.; Lecesne, A. Mechanisms of Resistance to Antibody-Drug Conjugates. *Int J Mol Sci* **2023**, *24*, doi:10.3390/ijms24119674.
54. Nagy, P.; Friedländer, E.; Tanner, M.; Kapanen, A.I.; Carraway, K.L.; Isola, J.; Jovin, T.M. Decreased accessibility and lack of activation of ErbB2 in JIMT-1, a herceptin-resistant, MUC4-expressing breast cancer cell line. *Cancer Res* **2005**, *65*, 473-482.
55. Carraway, K.L.; Perez, A.; Idris, N.; Jepson, S.; Arango, M.; Komatsu, M.; Haq, B.; Price-Schiavi, S.A.; Zhang, J.; Carraway, C.A. Muc4/sialomucin complex, the intramembrane ErbB2 ligand, in cancer and epithelia: to protect and to survive. *Prog Nucleic Acid Res Mol Biol* **2002**, *71*, 149-185, doi:10.1016/s0079-6603(02)71043-x.
56. Royce, M.; Osgood, C.L.; Amatya, A.K.; Fiero, M.H.; Chang, C.J.G.; Ricks, T.K.; Shetty, K.A.; Kraft, J.; Qiu, J.; Song, P.; et al. FDA Approval Summary: Margetuximab plus Chemotherapy for Advanced or Metastatic HER2-Positive Breast Cancer. *Clin Cancer Res* **2022**, *28*, 1487-1492, doi:10.1158/1078-0432.Ccr-21-3247.
57. Nordstrom, J.L.; Gorlatov, S.; Zhang, W.; Yang, Y.; Huang, L.; Burke, S.; Li, H.; Ciccarone, V.; Zhang, T.; Stavenhagen, J.; et al. Anti-tumor activity and toxicokinetics analysis of MGAH22, an anti-HER2 monoclonal antibody with enhanced Fcγ receptor binding properties. *Breast Cancer Res* **2011**, *13*, R123, doi:10.1186/bcr3069.
58. Rugo, H.S.; Im, S.A.; Cardoso, F.; Cortés, J.; Curigliano, G.; Musolino, A.; Pegram, M.D.; Wright, G.S.; Saura, C.; Escrivá-de-Romaní, S.; et al. Efficacy of Margetuximab vs Trastuzumab in Patients With Pretreated ERBB2-Positive Advanced Breast Cancer: A Phase 3 Randomized Clinical Trial. *JAMA Oncol* **2021**, *7*, 573-584, doi:10.1001/jamaoncol.2020.7932.
59. Mandó, P.; Rivero, S.G.; Rizzo, M.M.; Pinkasz, M.; Levy, E.M. Targeting ADCC: A different approach to HER2 breast cancer in the immunotherapy era. *Breast* **2021**, *60*, 15-25, doi:10.1016/j.breast.2021.08.007.
60. Ko, B.K.; Lee, S.Y.; Lee, Y.H.; Hwang, I.S.; Persson, H.; Rockberg, J.; Borrebaeck, C.; Park, D.; Kim, K.T.; Uhlen, M.; et al. Combination of novel HER2-targeting antibody 1E11 with trastuzumab shows synergistic antitumor activity in HER2-positive gastric cancer. *Mol Oncol* **2015**, *9*, 398-408, doi:10.1016/j.molonc.2014.09.007.
61. Yamada, S.; Itai, S.; Nakamura, T.; Chang, Y.W.; Harada, H.; Suzuki, H.; Kaneko, M.K.; Kato, Y. Establishment of H(2)Mab-119, an Anti-Human Epidermal Growth Factor Receptor 2 Monoclonal Antibody, Against Pancreatic Cancer. *Monoclon Antib Immunodiagn Immunother* **2017**, *36*, 287-290, doi:10.1089/mab.2017.0050.
62. Kaneko, M.K.; Yamada, S.; Itai, S.; Kato, Y. Development of an Anti-HER2 Monoclonal Antibody H2Mab-139 Against Colon Cancer. *Monoclon Antib Immunodiagn Immunother* **2018**, *37*, 59-62, doi:10.1089/mab.2017.0052.
63. Kato, Y.; Ohishi, T.; Takei, J.; Nakamura, T.; Sano, M.; Asano, T.; Sayama, Y.; Hosono, H.; Kawada, M.; Kaneko, M.K. An Anti-Human Epidermal Growth Factor Receptor 2 Monoclonal Antibody H2Mab-19 Exerts Antitumor Activity in Mouse Colon Cancer Xenografts. *Monoclon Antib Immunodiagn Immunother* **2020**, *39*, 123-128, doi:10.1089/mab.2020.0009.
64. Kato, Y.; Ohishi, T.; Yamada, S.; Itai, S.; Takei, J.; Sano, M.; Nakamura, T.; Harada, H.; Kawada, M.; Kaneko, M.K. Anti-Human Epidermal Growth Factor Receptor 2 Monoclonal Antibody H2Mab-41 Exerts Antitumor Activity in a Mouse Xenograft Model of Colon Cancer. *Monoclon Antib Immunodiagn Immunother* **2019**, *38*, 157-161, doi:10.1089/mab.2019.0017.
65. Kato, Y.; Ohishi, T.; Sano, M.; Asano, T.; Sayama, Y.; Takei, J.; Kawada, M.; Kaneko, M.K. H(2)Mab-19 Anti-Human Epidermal Growth Factor Receptor 2 Monoclonal Antibody Therapy Exerts Antitumor Activity in Pancreatic Cancer Xenograft Models. *Monoclon Antib Immunodiagn Immunother* **2020**, *39*, 61-65, doi:10.1089/mab.2020.0011.
66. Kato, Y.; Ohishi, T.; Takei, J.; Nakamura, T.; Kawada, M.; Kaneko, M.K. An Antihuman Epidermal Growth Factor Receptor 2 Monoclonal Antibody (H(2)Mab-19) Exerts Antitumor Activity in Glioblastoma Xenograft Models. *Monoclon Antib Immunodiagn Immunother* **2020**, *39*, 135-139, doi:10.1089/mab.2020.0013.
67. Azim, H.A.; Azim, H.A., Jr. Systemic treatment of brain metastases in HER2-positive breast cancer: current status and future directions. *Future Oncol* **2012**, *8*, 135-144, doi:10.2217/fon.11.149.
68. Leone, J.P.; Leone, B.A. Breast cancer brain metastases: the last frontier. *Exp Hematol Oncol* **2015**, *4*, 33, doi:10.1186/s40164-015-0028-8.

69. Turini, M.; Chames, P.; Bruhns, P.; Baty, D.; Kerfelec, B. A Fc γ RIII-engaging bispecific antibody expands the range of HER2-expressing breast tumors eligible to antibody therapy. *Oncotarget* **2014**, *5*, 5304-5319, doi:10.18632/oncotarget.2093.
70. Diermeier-Daucher, S.; Ortmann, O.; Buchholz, S.; Brockhoff, G. Trifunctional antibody ertumaxomab: Non-immunological effects on Her2 receptor activity and downstream signaling. *MAbs* **2012**, *4*, 614-622, doi:10.4161/mabs.21003.
71. Haense, N.; Atmaca, A.; Pauligk, C.; Steinmetz, K.; Marmé, F.; Haag, G.M.; Rieger, M.; Ottmann, O.G.; Ruf, P.; Lindhofer, H.; et al. A phase I trial of the trifunctional anti Her2 \times anti CD3 antibody ertumaxomab in patients with advanced solid tumors. *BMC Cancer* **2016**, *16*, 420, doi:10.1186/s12885-016-2449-0.
72. Schram, A.M.; Odintsov, I.; Espinosa-Cotton, M.; Khodos, I.; Sisso, W.J.; Mattar, M.S.; Lui, A.J.W.; Vojnic, M.; Shameem, S.H.; Chauhan, T.; et al. Zenocutuzumab, a HER2 \times HER3 Bispecific Antibody, Is Effective Therapy for Tumors Driven by NRG1 Gene Rearrangements. *Cancer Discov* **2022**, *12*, 1233-1247, doi:10.1158/2159-8290.Cd-21-1119.
73. Fontana, E.; Torga, G.; Fostea, R.; Cleator, S.; Wasserman, E.; Murat, A.; Arkenau, H.T. Sustained Tumor Regression With Zenocutuzumab, a Bispecific Antibody Targeting Human Epidermal Growth Factor Receptor 2/Human Epidermal Growth Factor Receptor 3 Signaling, in NRG1 Fusion-Positive, Estrogen Receptor-Positive Breast Cancer After Progression on a Cyclin-Dependent Kinase 4/6 Inhibitor. *JCO Precis Oncol* **2022**, *6*, e2100446, doi:10.1200/po.21.00446.
74. McDonagh, C.F.; Huhlov, A.; Harms, B.D.; Adams, S.; Paragas, V.; Oyama, S.; Zhang, B.; Luus, L.; Overland, R.; Nguyen, S.; et al. Antitumor activity of a novel bispecific antibody that targets the ErbB2/ErbB3 oncogenic unit and inhibits heregulin-induced activation of ErbB3. *Mol Cancer Ther* **2012**, *11*, 582-593, doi:10.1158/1535-7163.Mct-11-0820.
75. Chen, Y.L.; Cui, Y.; Liu, X.; Liu, G.; Dong, X.; Tang, L.; Hung, Y.; Wang, C.; Feng, M.Q. A bispecific antibody targeting HER2 and PD-L1 inhibits tumor growth with superior efficacy. *J Biol Chem* **2021**, *297*, 101420, doi:10.1016/j.jbc.2021.101420.
76. Gu, C.L.; Zhu, H.X.; Deng, L.; Meng, X.Q.; Li, K.; Xu, W.; Zhao, L.; Liu, Y.Q.; Zhu, Z.P.; Huang, H.M. Bispecific antibody simultaneously targeting PD1 and HER2 inhibits tumor growth via direct tumor cell killing in combination with PD1/PDL1 blockade and HER2 inhibition. *Acta Pharmacol Sin* **2022**, *43*, 672-680, doi:10.1038/s41401-021-00683-8.
77. Boulch, M.; Cazaux, M.; Loe-Mie, Y.; Thibaut, R.; Corre, B.; Lemaître, F.; Grandjean, C.L.; Garcia, Z.; Bousso, P. A cross-talk between CAR T cell subsets and the tumor microenvironment is essential for sustained cytotoxic activity. *Sci Immunol* **2021**, *6*, doi:10.1126/sciimmunol.abd4344.
78. Sureda, A.; Lugtenburg, P.J.; Kersten, M.J.; Subklewe, M.; Spanjaart, A.; Shah, N.N.; Kerbauy, L.N.; Roddie, C.; Pennings, E.R.A.; Mahuad, C.; et al. Cellular therapy in lymphoma. *Hematol Oncol* **2023**, doi:10.1002/hon.3200.
79. Shin, M.H.; Oh, E.; Kim, Y.; Nam, D.H.; Jeon, S.Y.; Yu, J.H.; Minn, D. Recent Advances in CAR-Based Solid Tumor Immunotherapy. *Cells* **2023**, *12*, doi:10.3390/cells12121606.
80. Mullard, A. FDA approves first CART therapy. *Nat Rev Drug Discov* **2017**, *16*, 669, doi:10.1038/nrd.2017.196.
81. Shiina, S.; Ohno, M.; Ohka, F.; Kuramitsu, S.; Yamamichi, A.; Kato, A.; Motomura, K.; Tanahashi, K.; Yamamoto, T.; Watanabe, R.; et al. CAR T Cells Targeting Podoplanin Reduce Orthotopic Glioblastomas in Mouse Brains. *Cancer Immunol Res* **2016**, *4*, 259-268, doi:10.1158/2326-6066.Cir-15-0060.
82. Ishikawa, A.; Waseda, M.; Ishii, T.; Kaneko, M.K.; Kato, Y.; Kaneko, S. Improved anti-solid tumor response by humanized anti-podoplanin chimeric antigen receptor transduced human cytotoxic T cells in an animal model. *Genes Cells* **2022**, *27*, 549-558, doi:10.1111/gtc.12972.
83. Fujii, Y.; Kaneko, M.K.; Kato, Y. MAP Tag: A Novel Tagging System for Protein Purification and Detection. *Monoclon Antib Immunodiagn Immunother* **2016**, *35*, 293-299, doi:10.1089/mab.2016.0039.
84. Fujii, Y.; Kaneko, M.K.; Ogasawara, S.; Yamada, S.; Yanaka, M.; Nakamura, T.; Saidoh, N.; Yoshida, K.; Honma, R.; Kato, Y. Development of RAP Tag, a Novel Tagging System for Protein Detection and Purification. *Monoclon Antib Immunodiagn Immunother* **2017**, *36*, 68-71, doi:10.1089/mab.2016.0052.
85. Ikota, H.; Nobusawa, S.; Arai, H.; Kato, Y.; Ishizawa, K.; Hirose, T.; Yokoo, H. Evaluation of IDH1 status in diffusely infiltrating gliomas by immunohistochemistry using anti-mutant and wild type IDH1 antibodies. *Brain Tumor Pathol* **2015**, *32*, 237-244, doi:10.1007/s10014-015-0222-8.
86. Kato, Y. Specific monoclonal antibodies against IDH1/2 mutations as diagnostic tools for gliomas. *Brain Tumor Pathol* **2015**, *32*, 3-11, doi:10.1007/s10014-014-0202-4.

87. Nanamiya, R.; Suzuki, H.; Takei, J.; Li, G.; Goto, N.; Harada, H.; Saito, M.; Tanaka, T.; Asano, T.; Kaneko, M.K.; et al. Development of Monoclonal Antibody 281-mG(2a)-f Against Golden Hamster Podoplanin. *Monoclon Antib Immunodiagn Immunother* **2022**, *41*, 311-319, doi:10.1089/mab.2021.0058.

Disclaimer/Publisher's Note: The statements, opinions and data contained in all publications are solely those of the individual author(s) and contributor(s) and not of MDPI and/or the editor(s). MDPI and/or the editor(s) disclaim responsibility for any injury to people or property resulting from any ideas, methods, instructions or products referred to in the content.